Proceedings of the 12th International Conference on
Aluminium Alloys, September 5-9, 2010, Yokohama, Japan

pp. 805-810

Mechanical Properties, Microstructure and Formability of Aluminum Alloys with Dispersed Nanoscale Quasicrystalline Particles

Masashi Fujita[1], Hisamichi Kimura[2], Akihisa Inoue[2]

[1]Honda R&D Co., Ltd. Automobile R&D Center, 4630 Shimotakanezawa, Haga-machi, Haga-gun, Tochigi, 321-3393, Japan

[2]Institute for Materials Research, Tohoku University, 2-1-1 Katahira, Aoba-ku, Sendai, 980-8577, Japan

The quasicrystalline single phase alloys cannot be applied as the structural materials due to their remarkably brittleness. However, the quasicrystalline phase shows excellent hardness and it is very stable at elevated temperatures. New aluminum-based alloys with good mechanical properties were developed in high Al concentration range of 91-95 at.% for Al-Fe-Cr-Ti-M systems by the dispersion of nanoscale quasicrystalline particles in Al phase (M: Co and Mo). Powder metallurgy (P/M) Al-Fe-Cr-Ti-M alloys were prepared by extruding gas and water atomized powders at 673K. The ultimate tensile strength of the P/M alloys was investigated at temperature from room temperature to 673K. The effect of adding elements, M was discussed in the viewpoint of stability of super-cooled liquid state and formation ability of quasicrystalline phase. The P/M Al-Fe-Cr-Ti-M alloys with dispersed nanoscale quasicrystalline particles exhibited ultimate tensile strength of 350MPa at 573K and 200MPa at 673K.

Furthermore, the formability of the alloy with dispersed quasicrystalline particles was evaluated by compression test of the extruded bar at elevated temperature. The extruded alloy bar could be compressed without crack.

These mechanical properties and formability at elevated temperatures are promising for the future extension of the new aluminum-based alloys to practical materials.

Keywords: aluminum-based alloy, quasicrystalline phase, powder metallurgy, high elevated-temperature strength.

1. Introduction

It is known that quasicrystalline (Q.C.) alloys with stoichiometric compositions have high Vickers hardness (*Hv*) and extremely brittle nature. For example, Hv is 1010 for the rapidly solidified (RS) Q.C. $Al_{77.5}Mn_{22.5}$ alloy[1)], 710 for the RS Q.C. $Al_{85.6}Cr_{15.4}$ alloy[1)] and 735 for the RS Q.C. $Al_{86}V_{14}$ alloy[2)]. These alloys also have high thermal stability. The volume fraction of the Q.C. particles decreases in order of Cr＞Mn＞V in the powder metallurgy (P/M) $Al_{93}Fe_3M_2Ti_2$ (M: V, Cr, Mn) alloys[3)]. There is a possibility of synthesizing a new material with high specific strength, high elevated-temperature strength and high wear resistance by dispersing Q.C. particles into fcc-Al phase. The P/M $Al_{94}V_4Fe_2$ and $Al_{93}Fe_3Cr_2Ti_2$ alloys containing quasicrystalline phase have high strength exceeding 580MPa[4)], high-elevated temperature strength exceeding 300MPa at 573K, and much better wear resistance than commercial A390 aluminum alloy[4)]. This paper presents the microstructure and mechanical properties of Al-Fe-Cr-Ti-M (M: Co and Mo) alloys produced by melt spinning technique and powder metallurgy technique.

2. Experimental procedures

The alloy ingots were prepared by arc melting pure metals where there purity is better than 99.85% in an argon atmosphere. From the ingots, RS alloys with a cross section of $0.02 \times 1mm^2$ were produced by a melt spinning technique. The ingots of powder metallurgy (P/M) alloys were prepared by induction melting in an argon atmosphere. Rapidly solidified (RS) powders were produced by high

pressure gas and water atomization process (SWAP)[5], followed by sieving into the sizes smaller than 150 μm. By using the conventional powder metallurgy technique, P/M Al-Fe-Cr-Ti-M alloys with a diameter of 10 mm and a length of 600 mm were produced by extrusion of the atomized powders[6]. The microstructures of RS and P/M alloys were examined by X-ray diffraction analysis and transmission electron microscopy (TEM). Tensile strength was measured at a strain rate of 4.0×10^{-4} s^{-1} in the temperature range from room temperature to 673 K with an Instron testing machine.

The formability of the alloy with dispersed quasicrystalline particles was evaluated by compression test of the extruded bar at elevated temperature. The strain rate is similar to commercial forging process (0.78 /s). The compressive stress was compared with that of the conventional aluminum alloy (A2618-T6). The structure of the compressed alloy was examined by X-ray diffraction analysis and transmission electron microscopy in the viewpoint whether the original dispersed quasicrystalline structure was maintained.

3. Results and Discussion

3.1 Microstructure of RS $(Al_{0.93}Fe_{0.03}Cr_{0.02}Ti_{0.02})_{100-x}M_x$ (M: Co and Mo, x=0, 2 and 3) alloy ribbons

Figure 1 shows X-ray diffraction patterns of the RS $(Al_{0.93}Fe_{0.03}Cr_{0.02}Ti_{0.02})_{100-x}Co_x$ (x=0, 2 and 3) alloy ribbons produced by a melt spinning technique at the copper roller circumferential velocity (*Vc*) of 40 m/s. The X-ray diffraction peaks broaden by adding cobalt element compared with $Al_{93}Fe_3Cr_2Ti_2$ alloy. The X-ray diffraction pattern shows an amorphous single phase when Co is added to 3 at% (x=3). This means that addition of cobalt stabilizes the super-cooled liquid state of Al-Fe-Cr-Ti alloy.

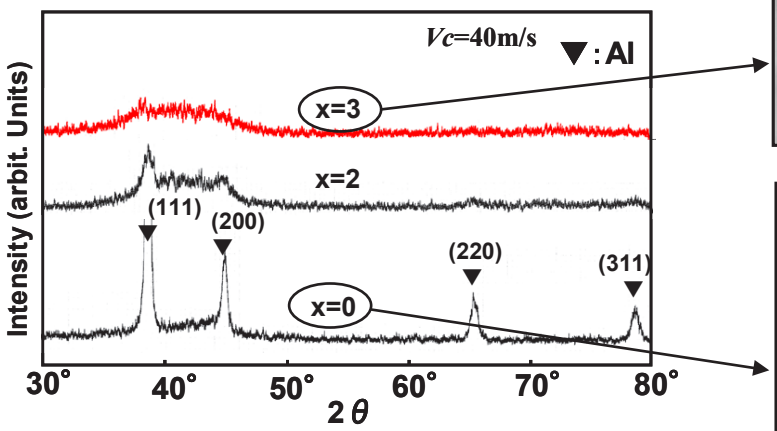

Fig. 1. X-ray diffraction patterns of the RS $(Al_{0.93}Fe_{0.03}Cr_{0.02}Ti_{0.02})_{100-x}Co_x$ alloys.

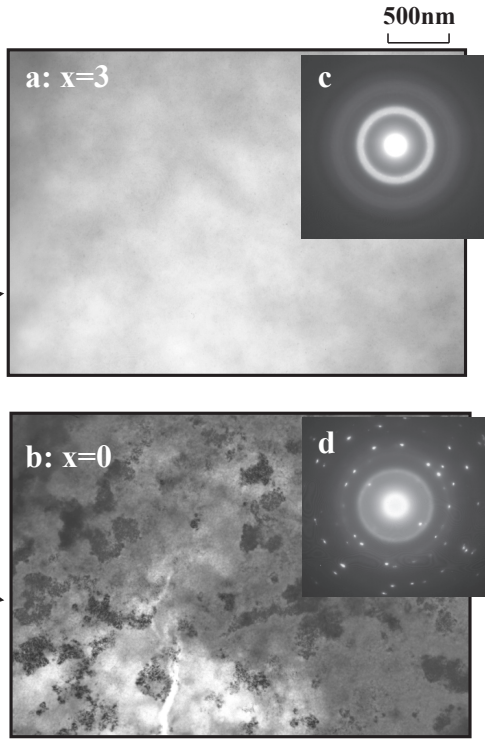

Fig. 2. Bright-field electron micrograph (a, b) and selected area electron diffraction pattern (c, d) of the RS $(Al_{0.93}Fe_{0.03}Cr_{0.02}Ti_{0.02})_{100-x}Co_x$ alloys.

Figure 2 shows bright-field electron micrographs (a, b) and selected area electron diffraction patterns (c, d) of the RS $(Al_{0.93}Fe_{0.03}Cr_{0.02}Ti_{0.02})_{100-x}Co_x$ (x=0 and 3). The electron micrograph (b) shows that the alloy consists of the mixed structure of amorphous and fcc-Al phase when cobalt is not added (x=0). One can see some segregation regions of fcc-Al phase with amrphous matrix in the micrograph. When cobalt is added to 3 at% (x=3), the electron micrograph (a) shows an amorphous

single phase corresponding to the result of X-ray diffraction analysis. The selected area electron diffraction pattern (c) shows also a typical harrow like pattern of amorphous single phase.

Figure 3 shows X-ray diffraction patterns of the RS $(Al_{0.93}Fe_{0.03}Cr_{0.02}Ti_{0.02})_{98}M_2$ (M=None, Mo) alloy ribbons produced by a melt spinning technique at the copper roller of *Vc*=20 m/s. The X-ray diffraction peaks of the $Al_{93}Fe_3Cr_2Ti_2$ alloy consist of fcc-Al, quasicrystalline (Q.C.) and $Al_{23}Ti_9$ phases. On the other hand, by addition of 2 at% Mo, the intermetallic compound peaks disappear and the quasicrystalline peaks becomes very clear. This means that molybdenum imparts a better formation ability of quasicrystalline phase to Al-Fe-Cr-Ti alloy. Figure 4 shows bright-field electron micrograph (a) and selected area electron diffraction pattern (b) of the RS $(Al_{0.93}Fe_{0.03}Cr_{0.02}Ti_{0.02})_{98}Mo_2$ alloy. Small particles 100nm or less in diameter are dispersed uniformly in the alloy. The selected area electron diffraction pattern from the particle shows a typical pattern of quasicrystalline phase along five-fold axes. This means these particles are quasicrystalline phases in the fcc-Al matrix.

In alloy design to disperse nanoscale Q.C. particles into fcc-Al phase, it is definitely important to consider the balance between the stability of super-cooled liquid state and the formation ability of quasicrystalline phase. In this study, Co and Mo are added to Al-Fe-Cr-Ti alloy to balance those two issues.

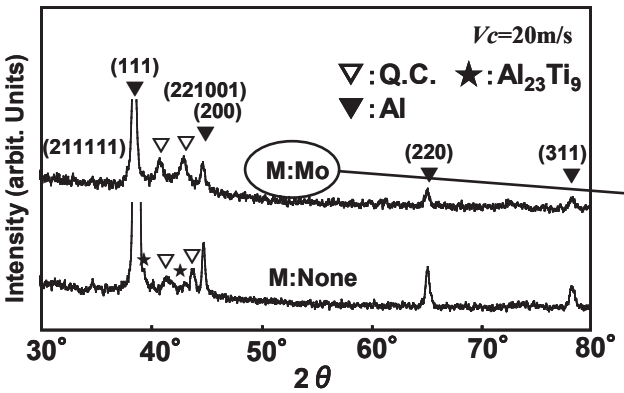

Fig. 3. X-ray diffraction patterns of the RS $(Al_{0.93}Fe_{0.03}Cr_{0.02}Ti_{0.02})_{98}M_2$ alloys

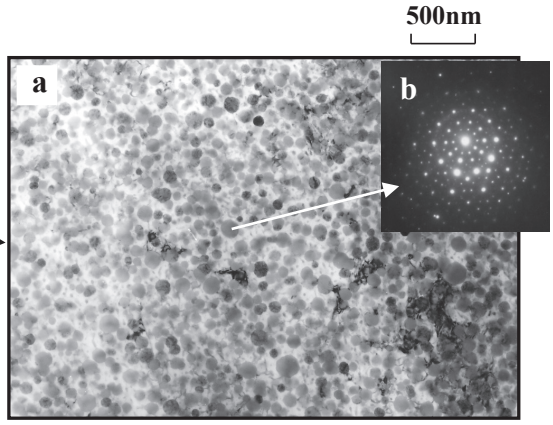

Fig. 4. Bright-field electron micrograph (a) and selected area electron diffraction pattern (b) of the RS $(Al_{0.93}Fe_{0.03}Cr_{0.02}Ti_{0.02})_{98}Mo_2$ alloy.

3.2 Microstructure and mechanical properties of P/M $Al_{93}Fe_{2.45}Cr_{2.45}Mo_{0.5}Ti_{0.8}Co_{0.8}$ alloy

The atomaized alloy powder was produced by high-pressure spinning water atomization process called SWAP, shown in figure 5. This process is the two-staged atomization process, where the molten alloy is divided by N_2 gas at first, and then cooled rapidly in spinning water.

Figure 6 shows bright field electron micrograph (a) and selected-area electron diffraction pattern (b) of the P/M $Al_{93}Fe_{2.45}Cr_{2.45}Mo_{0.5}Ti_{0.8}Co_{0.8}$ alloy. One can see the spherical Q.C. particles with a grain size of about 100 nm dispersed uniformly into fcc-Al matrix after extrusion process.

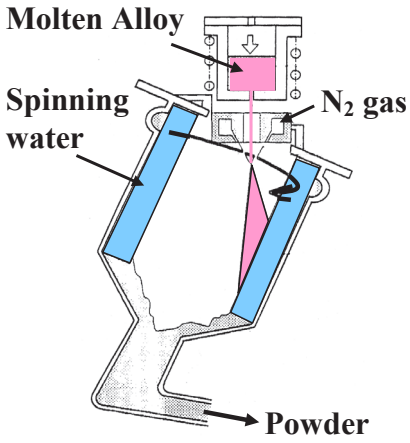

Fig. 5. SWAP process

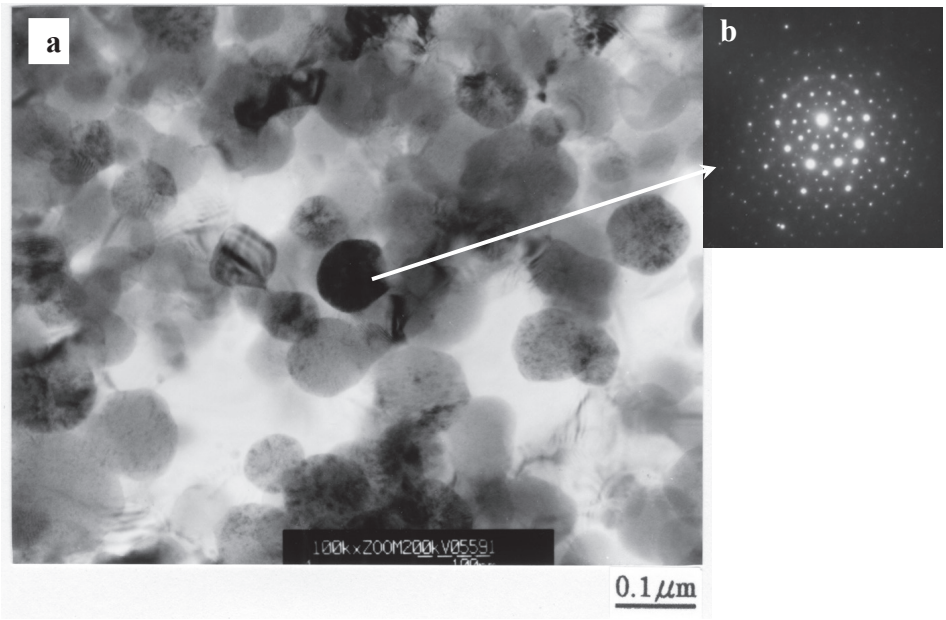

Fig. 6. Bright field electron micrograph and selected-area electron diffraction pattern of the P/M $Al_{93}Fe_{2.45}Cr_{2.45}Mo_{0.5}Ti_{0.8}Co_{0.8}$ alloy.

Figure 7 shows the temperature dependence of the ultimate tensile strength (σ_{uts}) for the P/M $Al_{93}Fe_{2.45}Cr_{2.45}Mo_{0.5}Ti_{0.8}Co_{0.8}$ alloy at each testing temperature, together with the data of $Al_{93}Fe_3Cr_2Ti_2$ alloy and the conventional Al-based alloy. The σ_{uts} shows much higher ones over the whole temperature range up to 673 K as compared with those of conventional Al alloys with high elevated temperature strength. This outstanding tensile strength at elevated temperature is based on uniform dispersion of the quasicrystalline particles excellent in thermal stability.

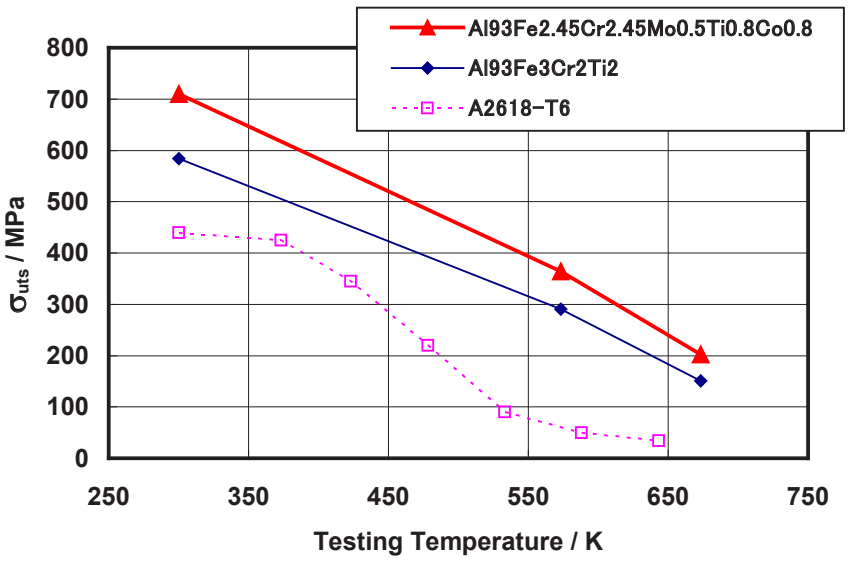

Fig. 7. Temperature dependence of ultimate tensile strength (σ_{UTS}) as a function of testing temperature for the P/M $Al_{93}Fe_{2.45}Cr_{2.45}Mo_{0.5}Ti_{0.8}Co_{0.8}$ alloy.

3.3 Formability of P/M $Al_{93}Fe_{2.45}Cr_{2.45}Mo_{0.5}Ti_{0.8}Co_{0.8}$ alloy

The formability of P/M $Al_{93}Fe_{2.45}Cr_{2.45}Mo_{0.5}Ti_{0.8}Co_{0.8}$ alloy was evaluated by compression test of the extruded bar at elevated temperature of 673K. Figure 8 shows the testing condition of the compression test. The testing temperature was set at 673K, which was similar to forging temperature of the commercial aluminum alloy. The strain rate is similar to that of commercial forging process (0.78 /s). Figure 9 shows the appearances of compressed specimens with compressive strain of 60%. Figure 9-(a) shows the axial compression of the extruded bar. Figure 9-(b) shows the compression of the radial direction of the extruded bar. The both extruded bars can be compressed without crack. Due to their high elevated temperature strength, the compressive stress is about three times higher over the whole strain range, as compared with those of conventional aluminum-based alloy.

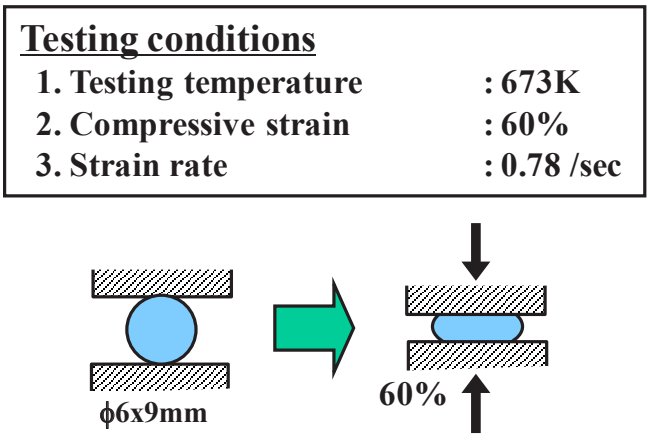

Fig. 8. Testing conditions of compression test

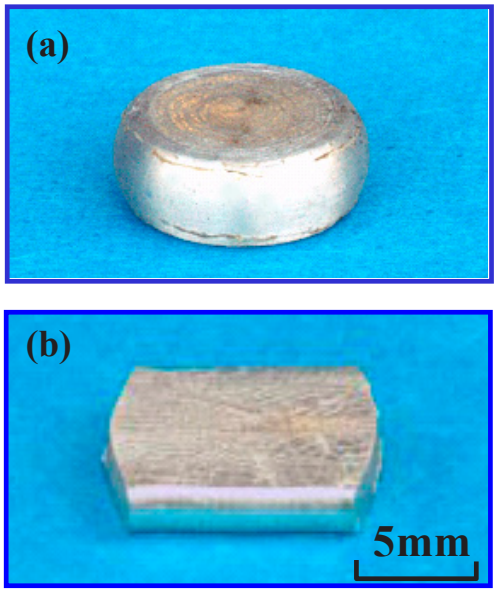

Fig. 9. Appearance of compressed specimens

Figure 10 shows X-ray diffraction patterns of the P/M $Al_{93}Fe_{2.45}Cr_{2.45}Mo_{0.5}Ti_{0.8}Co_{0.8}$ alloy with the as-extruded one and the compressed one. The XRD peaks of both alloys correspond to fcc-Al and QC phases.

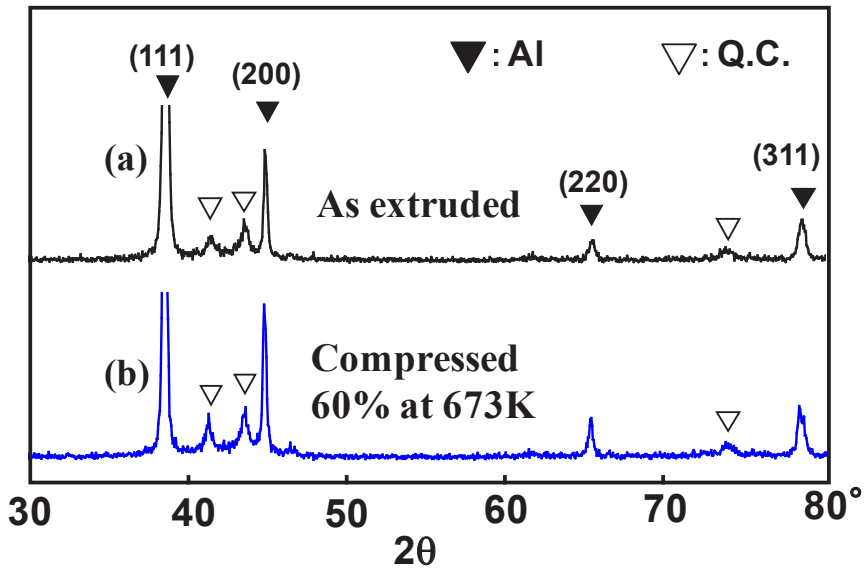

Fig. 10. X-ray diffraction patterns of the P/M $Al_{93}Fe_{2.45}Cr_{2.45}Mo_{0.5}Ti_{0.8}Co_{0.8}$ alloys.

Figure 11 shows the bright-field electron micrographs of the P/M $Al_{93}Fe_{2.45}Cr_{2.45}Mo_{0.5}Ti_{0.8}Co_{0.8}$ alloy; as extruded one (a) and the compressed one (b) . The structure of the alloy with dispersed nanoscale quasicrystalline particles is maintained even after compression test at 673K. The factor maintaining the structure after the compression test at the elevated temperature depends on the balance of thermally stable and hard quasicrystalline particles and relatively soft fcc-aluminum matrix.

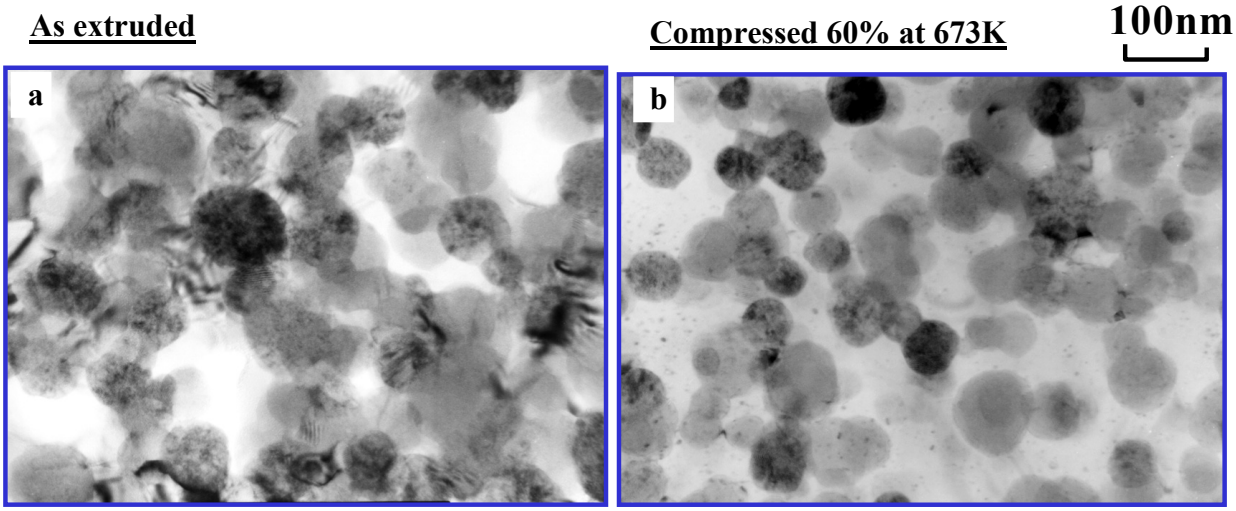

Fig. 11. Bright field electron micrographs of the P/M $Al_{93}Fe_{2.45}Cr_{2.45}Mo_{0.5}Ti_{0.8}Co_{0.8}$ alloy; as extruded one (a) and the compressed one (b)

This fact has suggested the manufacturing possibility of the novel forging parts with superior strength at elevated temperature. These mechanical properties and formability at elevated temperatures are promising for the future extension of the new aluminum-based alloys to practical materials.

4. Summary

By addition of Co and Mo to Al-Fe-Cr-Ti alloy, the good balance between the stability of super-cooled liquid state and the formation ability of quasicrystalline phase was obtained. The P/M Al-Fe-Cr-Ti-Co-Mo alloy with dispersed nanoscale quasicrystalline particles exhibited ultimate tensile strength of more than 350 MPa at 573 K and 200 MPa at 673 K. The alloy had excellent formability at elevated temperature with maintaining its structure of dispersed nanoscale quasicrystalline particles.

5. References

[1] A. Inoue, J. Mater. Sci., 22 (1987), 1758.
[2] H. M. Kimura, J. Jpn. Inst. Light Met., 48 (1988), 127.
[3] H. M. Kimura, J. Jpn. Soc. Powder Met., 46 (1999), 1321.
[4] H. M. Kimura, Mater. Trans. JIM, 41 (2000), 1550.
[5] K. Ichikawa, Metals, 65 (1995), 1165.
[6] H. M. Kimura, J. Jpn. Soc. Powder Met., 56 (2009), 697.